ORIGINAL ARTICLE

Vessel Dilation Attenuates Endothelial Dysfunction Following Middle Cerebral Artery Occlusion in Hyperglycemic Rats

Zhi-Hao Mu,[1] Zhen Jiang,[1] Xiao-Jie Lin,[2] Li-Ping Wang,[1] Yan Xi,[2,3] Zhi-Jun Zhang,[2] Yong-Ting Wang[2],* & Guo-Yuan Yang[1,2],*

1 Department of Neurology, Ruijin Hospital, School of Medicine, Shanghai Jiao Tong University, Shanghai, China
2 Med-X Research Institute and School of Biomedical Engineering, Shanghai Jiao Tong University, Shanghai, China
3 Center for Biotechnology and Interdisciplinary Studies, Department of Biomedical Engineering, Rensselaer Polytechnic Institute, Troy, NY, USA

SUMMARY

Objectives: Dynamically observe cerebral vascular changes in hyperglycemic rats *in vivo* and explore the effect of diabetes on endothelial function after ischemic stroke. **Background:** Diabetes affects both large and small vessels in the brain, but the dynamic process and mechanism are unclear. **Methods:** We investigated the structural and functional changes of brain vasculature in living hyperglycemic rats and their impact on stroke outcomes via a novel technique: synchrotron radiation angiography. We also examined the effect of prolonged fasudil treatment on arterial reactivity and hemorrhagic transformation. Adult Sprague Dawley rats were treated by streptozotocin to induce type 1 diabetes. These hyperglycemic rats received fasudil pretreatment and then underwent transient middle cerebral artery occlusion. **Results:** We found that diabetes caused arteries narrowing in the circus Willis as early as 2 weeks after streptozotocin injection ($P < 0.05$). These vessels were further constricted after middle cerebral artery occlusion. L-NAME could induce regional constrictions and impaired relaxation in hyperglycemic animals. Furthermore, hemorrhagic transformation was also increased in the hyperglycemic rats compared to the control ($P < 0.05$). In fasudil-treated rats, the internal carotid artery narrowing was ameliorated and L-NAME-induced regional constriction was abolished. Importantly, stroke prognosis was improved in fasudil-treated rats compared to the control ($P < 0.05$). **Conclusions:** Our dynamic angiographic data demonstrated that diabetes could impair the cerebral arterial reactivity. Prolonged fasudil treatment could attenuate arterial dysfunction and improve the prognosis of ischemic stroke by affecting both the large and small vasculature.

Introduction

Diabetes is an important risk factor for stroke. The incidence of ischemic stroke in diabetic patients is about twofold to sixfold higher than patients without diabetes [1]. In addition, the occurrence of hemorrhagic transformation following r-tPA treatment after ischemic stroke is much higher in diabetic patients [2]. Diabetic patients also have poorer prognosis during recovery phase after ischemia [3].

Even though it is known that diabetes affects cerebrovasculature [4], it is unclear how pre-existing vascular structural and functional changes caused by diabetes impact on cerebral perfusion and progression after stroke in real time. Diabetic vascular dysfunction has been recognized as a vital mechanism contributing to the progression of stroke [5–7]. Clinical investigations have shown that vascular dysfunction is an independent predictor of cardiovascular events [8–10]. Experimental studies also showed that diabetes impairs the dilation of cerebral macro and microvessels

[11,12], which hindered compensatory collateral artery recruitment and vasodilation after ischemia [7,13]. Therapeutic regulation of vascular dysfunction could increase cerebral blood flow and improve stroke outcome. Although many studies have revealed vascular dysfunction in cortical arterioles, basilar [14], and carotid arteries [15], our knowledge of vascular dysfunction is refined to local and separated vessels, partly due to the lacking of techniques to image brain cerebrovasculature in larger scale. Synchrotron radiation X-ray angiography (SRA), as a novel technique to visualize cerebral vasculature, has been developed recently [16]. It was used to study macro- and microvascular changes in coronary vessels *in vivo*, which suggests its potential in probing cerebrovascular dysfunction in the early phase of diabetes [17].

Recent studies have shown that RhoA/Rho-kinase activity is increased both in diabetes and in stroke, which could contribute to increased vascular tone and decreased nitric oxide production [18]. It was found that enhanced activity of Rho-kinase was associated with impaired endothelium-dependent responses [19],

neutrophil-induced endothelial apoptosis [20], and blood–brain barrier damage [21]. In contrast, inhibition of rho-kinase could prevent vascular dysfunction [22], augment blood flow in cerebral ischemia [23,24], and maintain blood–brain barrier integrity [25]. Although previous studies have confirmed that prolonged inhibition of rho-kinase could attenuate vascular contractility [26] and maintain endothelial function [20], there are few studies that clarify its effects in diabetic cerebral complications.

In this study, we explored the diabetes-induced cerebrovascular changes in deep brain vessels and its impact on stroke prognosis using dynamic synchrotron radiation X-ray angiography. We tested whether prolonged inhibition of Rho-kinase by fasudil, a selective RhoA/Rho-kinase inhibitor, could ameliorate diabetes-induced vascular dysfunction and improve the prognosis of stroke.

Materials and Methods

Induction of hyperglycemia and Fasudil Treatment

Animal experiment protocols were approved by the Institutional Animal Care and Use Committee of the School of Biomedical Engineering, Shanghai Jiao Tong University, Shanghai, China (Permission number: Bioethics 2012022). This manuscript is compliant with the animal research: reporting *in vivo* experiments guidelines. Fifty-four adult male Sprague Dawley rats (Sippr-BK, Shanghai, China) were divided into three groups: nonhyperglycemic (n = 16), hyperglycemic (n = 22), and fasudil-treated hyperglycemic groups (n = 16). Hyperglycemia was induced in rats weighing 250–300 g by a bolus intraperitoneal injection of streptozotocin (STZ, 60 mg/kg in citrate buffer, Sigma, St. Louis, MO, USA), while nonhyperglycemic group received buffer only. The fasting blood glucose level was tested 1 week after STZ injection and again at 1 day before transient middle cerebral artery occlusion (MCAO) using a glucose analyzer (Bayer, Leverkusen, Germany). Hyperglycemic rat was defined by a fasting blood glucose concentration of over 15 mmol/L.

Fasudil-treated hyperglycemic group received intraperitoneal fasudil daily (10 mg/kg, Chase Sun, Tianjin, China) from 1 week after STZ administration to 2 days before transient middle cerebral artery occlusion (tMCAO), a total of 19 days of treatment. Nonhyperglycemic control and hyperglycemic group were treated with the same amount of normal saline. Mean arterial blood pressure was measured using the Visitech BP-2000 system (Visitech Systems, Apex, NC, USA) before tMCAO.

Transient Middle Cerebral Artery Occlusion

The animals were subjected to tMCAO 27 days after hyperglycemia induction. The surgical procedure for tMCAO has been previously described [27]. Briefly, rats were anaesthetized by inhalation of isoflurane (2%, Abbot, Shanghai, China). Animals were then positioned supinely on a heating pad (RWD Life Science, Shenzhen, China) maintaining body temperature at 37 ± 0.5°C. The left common carotid artery (CCA), external carotid artery (ECA), and pterygopalatine artery (PPA) were isolated under an operating microscope (Leica; Wetzlar, Germany). A silicone-coated 4-0 suture (Dermalon, 1756-31, Covidien, Mansfield, MA, USA) was gently inserted from the ECA stump to the internal carotid artery (ICA) until it blocked the opening of the middle cerebral artery (MCA). The success of occlusion was assessed by a decrease of cerebral blood flow to less than 20% of the baseline using Laser Doppler flowmetry (Moor Lab; Moor Instruments, Axminster, UK). After 90 min of ischemia, the suture was carefully withdrawn and reperfusion was assessed by the restoration of cerebral blood flow.

Angiography Protocol

Synchrotron radiation X-ray angiography (SRA) was conducted at 1 day after tMCAO at beamline BL13W in Shanghai Synchrotron Radiation Facility (SSRF). Imaging setup and procedures have been described previously [16]. Briefly, the average beam current was 245 mA, and X-ray energy was 33.3 keV. Animals were anaesthetized by ketamine/xylazine (100 mg/10 mg/kg, intraperitoneally) during the imaging process. A PE-10 tube was inversely inserted into the ECA for injecting contrast agent. The rat was placed perpendicular to the beam, and iodinated contrast medium (Ipamiro, Shanghai, China) was injected into the CCA as a bolus (160 μL at 100 μL/second) using an automated microsyringe pump (LSP01-1A, Longer; Baoding, China). An X-ray complementary metal oxide semiconductor (pixel size of 6.5 × 6.5 μm, frame frequency of 30 Hz, Hamamatsu Ltd., Hamamatsu City, Japan) was used to record high-resolution real-time angiographic images at a distance of 650 mm to the sample. Contrast agent was administrated through external carotid artery by a bolus injection (160 μL within 2 seconds) in our study. It was noted that arterial administration was also adopted by another group and they found that bolus injection did not cause a significant pressure perturbation during image sequences [17].

After imaging baseline vasculature, Nω-nitro-l-arginine methyl ester (L-NAME; 50 mg/kg intravenous. bolus) was injected through tail vein to inhibit nitric oxide synthase (NOS) and angiographic images were taken at 5 min, 15 min, and 30 min after injection. Then fasudil (10 mg/kg iv. bolus) was also injected through tail vein as a vasodilator and rats were imaged at 5, 15, and 30 min after injection.

Assessment of Vessel Internal Diameter and Cortical Vascular Density

Measurements of vessel internal diameter (ID) of the circus Willis were conducted using image analysis software (ImageJ, National Institutes of Health, Bethesda, MD, USA). Vessel ID represents the average of three independent measurements. Arterial stenosis was defined as a decrease of arterial diameter to less than 70% of average arterial diameter of normal Sprague Dawley rats.

To assess cortical microvascular perfusion, we measured the vessel density of the perfusion angiogram. A short program written in Matlab (MathWorks, Natick, MA, USA) was used to identify perfused vessels from original SRA images. Briefly, identical areas covering the cortical branches of MCA were selected. Then, all angiographic images were de-noised under a same threshold to obtain a legible vessel map. The vessel density was defined as the percentage of pixels of vessels in total pixels of each identical area. The vessel signals in each area were summed and compared.

Measurements of Brain Lesion and Hemorrhage Volume

The brains were transcardially perfused with saline and fixed by 4% paraformaldehyde before being removed to freeze in −80°C isopentane. A series of 20-μm-thick coronal sections were cut and mounted on slides, with an interval of 200 μm between each section. A total of 15–39 frozen sections from each rat were stained with cresyl violet (Sigma) and delineated by ImageJ. Lesion volume between two adjacent sections was then calculated as Equation 1. The hemorrhage volume was evaluated by photographing the coronal sections as the same intervals as the lesion volume including a ruler in the field as a reference. And the hemorrhagic area of each section was measured with ImageJ and calculated using Equation 1. Total lesion and hemorrhage volume were derived as the sum of all volumes between each adjacent section and presented as a percentage of the lesion ratio compared with the contralateral hemisphere.

$$V = \frac{1}{3} \times h \times (S_1 + S_2 + \sqrt{S_1 \times S_2}) \tag{1}$$

Histology and Immunohistochemistry

Three consecutive sections with 200-μm intervals covering the ICA branch were stained with hematoxylin and eosin according to previously reported protocol [28]. Immunohistochemical staining was conducted against rat-specific smooth muscle cell α-actin (SMA, 1:50, Abcam, Cambridge, UK) to assess ICA smooth muscle cell phenotype. Brain sections were incubated with 4% paraformaldehyde for 5 min and permeabilized with 0.1% Triton X-100 for 30 min at room temperature. After blocking with 10% bovine serum albumin for 30 min, the brain sections were stained with SMA at 4°C overnight. Sections were rinsed with PBS and incubated with secondary antibody for 1 h. Slides were then visualized with a fluorescent microscope (Leica).

Statistical Analysis

Data were presented as mean ± SD and percentage. Media thickness, cross-sectional area, lesion, and hemorrhage volume were assessed with an unpaired Student's *t*-test using SPSS 16.0 (SPSS Inc, Armonk, NY, USA). One-way ANOVA was carried out to assess within-group differences of arterial diameters, followed by a two-tailed Student's *t*-test to determine statistical significance. A probability value of $P < 0.05$ was considered significant.

Results

Animal Characteristics

The body weight of hyperglycemic rats significantly decreased after STZ administration (Table 1, $P < 0.01$). Blood glucose significantly increased at 2 weeks after STZ administration compared to nonhyperglycemic control ($P < 0.01$) and maintained at a high

Table 1 Animal characteristics in control and hyperglycemic rats

	Control	DM2W	DM4W	DM6W
Body weight (g)	328 ± 33	256 ± 27*	257 ± 39*	264 ± 41*
Blood glucose (mmol/L)	5.9 ± 0.9	23.3 ± 3.1*	23.1 ± 2.0*	26.2 ± 3.2*
MAP (mmHg)	98 ± 7	94 ± 11	85 ± 10*†	84 ± 7*†

n = 10 per group. Values expressed as mean ± SD. MAP indicates mean arterial pressure. *Indicates $P < 0.01$ when compared to control group. †Indicates $P < 0.01$ when compared to DM2W group.

level until 6 weeks. Mean arterial pressure did not decrease until 4 weeks after STZ administration ($P < 0.01$).

Fasudil Preserved Endothelial Function in Hyperglycemic Rats

Vascular diameters of each primary branches of the circus Willis were measured from SRA images (Figure 1A). The diameters of ICA, MCA, PCA, and ACA in hyperglycemic rats decreased significantly compared to nonhyperglycemic control. Fasudil treatment did not affect these diameters (Figure 1B). The percentage of ICA stenosis progressed from 2 weeks (19%) to 6 weeks (38%) after STZ administration (Figure 1C). NOS inhibitor L-NAME was used to test the vascular constriction and relaxation function, and SRA showed that the vessels of the circus Willis exhibited general constriction with multiple marked focal constrictions after L-NAME administration in hyperglycemic rats. In contrast, in fasudil-treated group, the vessels of the circus Willis constricted without apparent focal constrictions (Figure 1D). Vasodilator could reverse focal constriction in hyperglycemic rats.

Fasudil Treatment Improved Stroke Prognosis in Hyperglycemic Rats

Hyperglycemic rats exhibited adverse prognosis after tMCAO compared to nonhyperglycemic control and fasudil treatment improved stroke outcome. The mortality rate of hyperglycemic rats after tMCAO is 23%, comparing to 0% in nonhyperglycemic control, while it decreased to 11% in fasudil-treated group. Lesion volume also increased significantly in hyperglycemic rats and fasudil treatment reduced lesion volume (Figure 2A,B). About 73% of hyperglycemic rats exhibited intracranial hemorrhage after tMCAO, compared to 0% in nonhyperglycemic control rats, and the hemorrhage volume of hyperglycemic rats was 142.7 ± 54.2 μm^2. In fasudil-treated group, hemorrhage rate was 43% and hemorrhage volume was 27.2 ± 19.2 μm^2 (Figure 2C,D).

Fasudil Treatment Ameliorated Ischemia-Induced Arterial Constrictions in Hyperglycemic Rats

To explore the vascular changes that underlie adverse stroke prognosis of hyperglycemic rats, we performed SRA at 1 day after
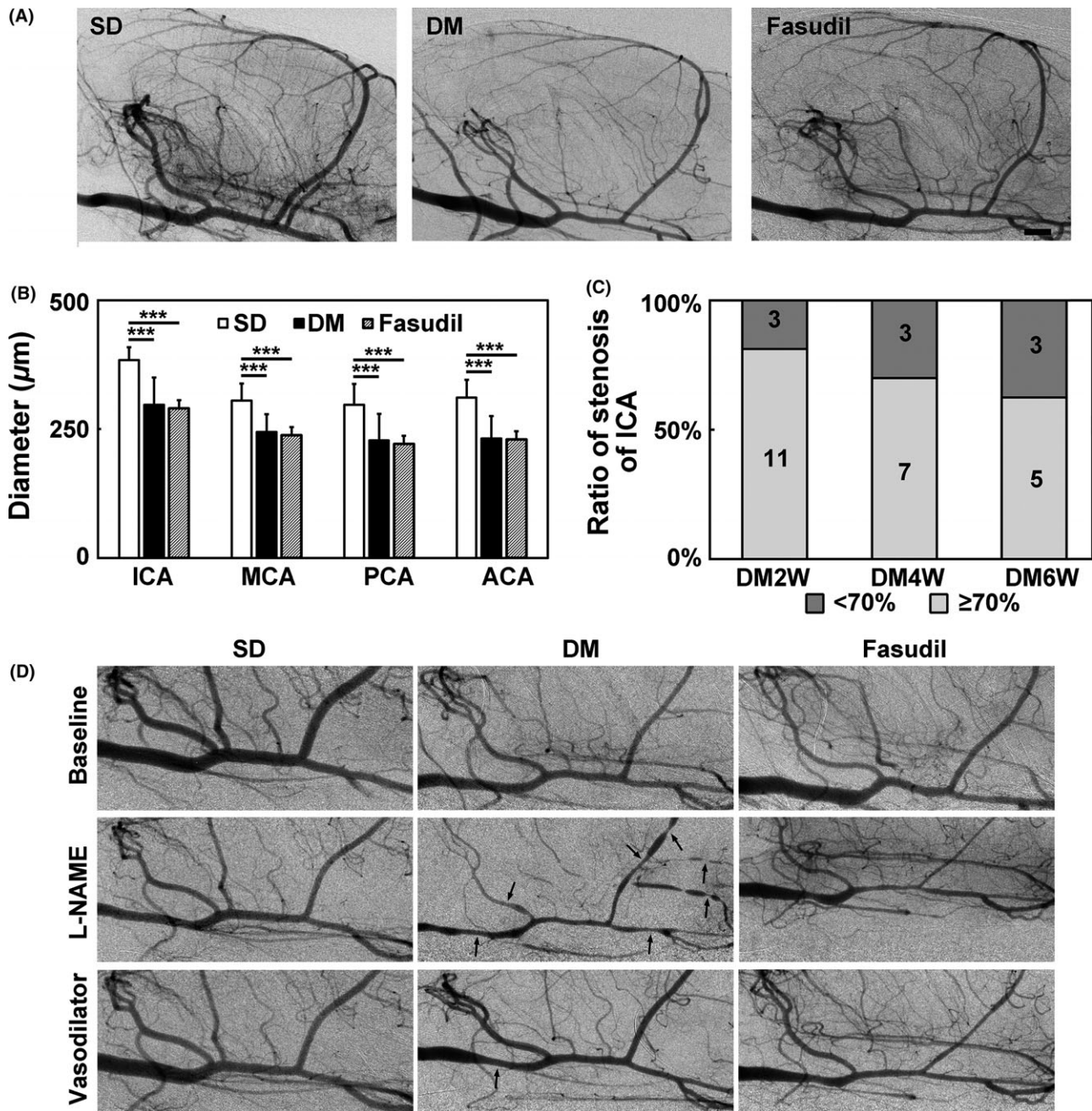
Figure 1 Fasudil preserved endothelial function in hyperglycemic rats. (**A**) Synchrotron radiation angiogram (SRA) images of the SD, hyperglycemic and fasudil-treated hyperglycemic rats. (**B**) Bar graph of arterial diameters of ICA, MCA, PCA, and ACA in SD, hyperglycemic, and fasudil-treated hyperglycemic rats. n = 7–8 per group, values are mean ± SD, ***$P < 0.001$, compared with SD. (**C**) Percentage of arterial stenosis of ICA in DM2W, DM4W, and DM6W rats, which represent for 2, 4, 6 weeks after hyperglycemia induction. (**D**) SRA images of the SD, hyperglycemic and fasudil-treated hyperglycemic rats before intervention, after L-NAME and vasodilator fasudil injection. Black arrow points to focal constrictions. Bar = 1 mm.

tMCAO and measured vascular diameters of ICA, MCA, PCA, and ACA in nonhyperglycemic, hyperglycemic, and fasudil-treated hyperglycemic rats. Results showed that hyperglycemic rats had significantly smaller vascular diameters compared to nonhyperglycemic control after tMCAO. ICA diameter was larger in fasudil-treated hyperglycemic rats than that in hyperglycemic rats

(Figure 3A,B), while the diameters of other vessels were not significantly different between the two groups. Comparison of ICA diameters before and after tMCAO showed that ICA diameter of hyperglycemic rats decreased after tMCAO, while that of the nonhyperglycemic and fasudil-treated rats remain unchanged (Figure 3C). Some hyperglycemic rats showed extreme constrictions
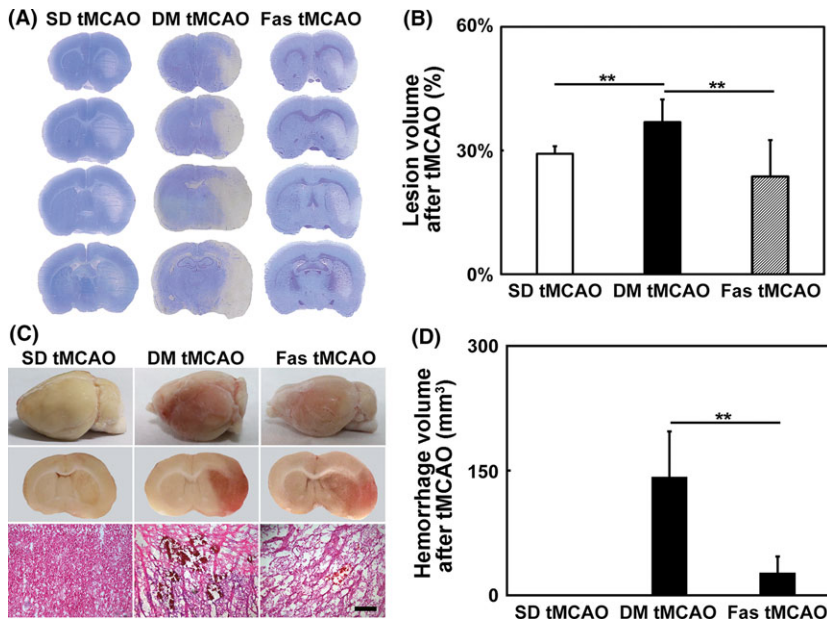
Figure 2 Fasudil treatment improved stroke prognosis in hyperglycemic rats. (**A**) Cresyl violet stained coronary sections of rat brain at 1 day after transient middle cerebral artery occlusion (tMCAO) in the SD, hyperglycemic and fasudil-treated hyperglycemic rats. (**B**) Bar graph of the infarct volumes in SD, hyperglycemic and fasudil-treated hyperglycemic rats. The three groups were abbreviated as SD tMCAO, DM tMCAO, and Fas tMCAO. n = 6–9 per group, values are mean ± SD, **$P < 0.01$, SD tMCAO versus DM tMCAO, DM tMCAO versus Fas tMCAO. (**C**) Pictures of whole brain, coronary sections of brain and H&E staining showed hemorrhage. (**D**) Bar graph of the hemorrhage volume in the SD rats, hyperglycemic and fasudil-treated hyperglycemic rats. n = 6–9 per group, values are mean ± SD, **$P < 0.01$, DM tMCAO versus Fas tMCAO. Bar = 200 μm.

of ICA and the lowest diameter was 105 μm, comparing to 384 μm in the normal control. H&E staining of ICA in hyperglycemic rats showed that the media–intima was thicker than that in nonhyperglycemic control (9.8 ± 1.0 μm vs. 6.4 ± 0.8 μm). Fasudil treatment reduced media–intima thickness to 7.2 ± 1.1 μm (Figure 3E). The inner diameter of ICA measured using H&E stained images was consistent with that measured using SRA images (Figure 3F).

Fasudil Treatment Preserved Endothelial Function and Maintained Cortical Perfusion after tMCAO

To investigate the dysfunction of vascular contraction and relaxation underlying hyperglycemic rats after tMCAO, we used L-NAME to probe vascular function. Blockade of NOS only caused a slight decrease in vessel diameter in control group, while it evoked focal constrictions in ICA in the hyperglycemic group. In addition, L-NAME caused reduced vessel density in hyperglycemic rats, while nonhyperglycemic- and fasudil-treated group both maintained the opening of cerebral vessels (Figure 3G). Immunostaining of ICA from both groups *in vitro* with SMA and DAPI showed that the morphology of smooth muscle cell transformed from spindle into elliptical shape, while the numbers of cell layers remained the same (Figure 3H). Perfused vessel density of hyperglycemic rats in cortex was much lower than control, while fasudil treatment increased cortical vessel density of hyperglycemic rats (Figure 4A,B).

Discussion

Our results revealed arterial stenosis and dysfunction of contractions/relaxations in the early stage of diabetes, which contributed to worsen prognosis after ischemic stroke. Prolonged fasudil treatment ameliorated diabetes-induced vascular dysfunction and

improved stroke prognosis. Our data is the first to evaluate deep brain cerebrovascular function in the early stage of diabetes and explore its role in stroke in living animals. Importantly, our results tested the possibility of preserving cerebrovascular function to improve the prognosis of diabetic stroke.

Due to the difference of derivation, duration, and blood glucose concentration among *in vitro* studies, the results about diabetes-induced cerebrovascular myogenic tone and reactivity changes were controversial. The PCA of normoglycemic rat was reported to have decreased myogenic tone when exposed to high glucose concentration [29], while others reported that myogenic tone increased in PCA from type 2 diabetic rats [30]. Our research found that diabetic rats exhibited lower baseline vessel inner diameter and focal constrictions after NOS inhibition, supporting that diabetes contributed to higher myogenic tone and reactivity in deep brain vessels [31]. While in contrast to previous results that oxygen–glucose deprivation reduced myogenic tone and slight reduction of the diameter of MCA in diabetic rats [31], we found that stroke induced significant reduction of arterial diameters in ICA, MCA, PCA, and ACA. Diabetic vascular dysfunction was characterized by impaired cerebral vasoreactivity. We found that focal constrictions under vascular modulators could be another marker. Histological analysis of the vessels showed that media–intima thickness of ICA increased, while cross-sectional area remains unchanged (data not shown). This suggests that the stenosis of ICA might reflect real-time arterial constrictions of the vessel other than increased thickness of the vessel wall.

Many studies indicated that type 1 diabetes showed impaired NOS-dependent dilation of cerebral arterioles [32,33]. Furthermore, diabetes-induced vascular dysfunction is critical to the prognosis of stroke [7,11,19] and chronic resveratrol treatment, losartan, and exercise training [34–36] restored NOS-dependent vascular dilation in type 1 diabetes and even lessened ischemia-induced brain injury in type 1 diabetes [37,38]. In our study, we
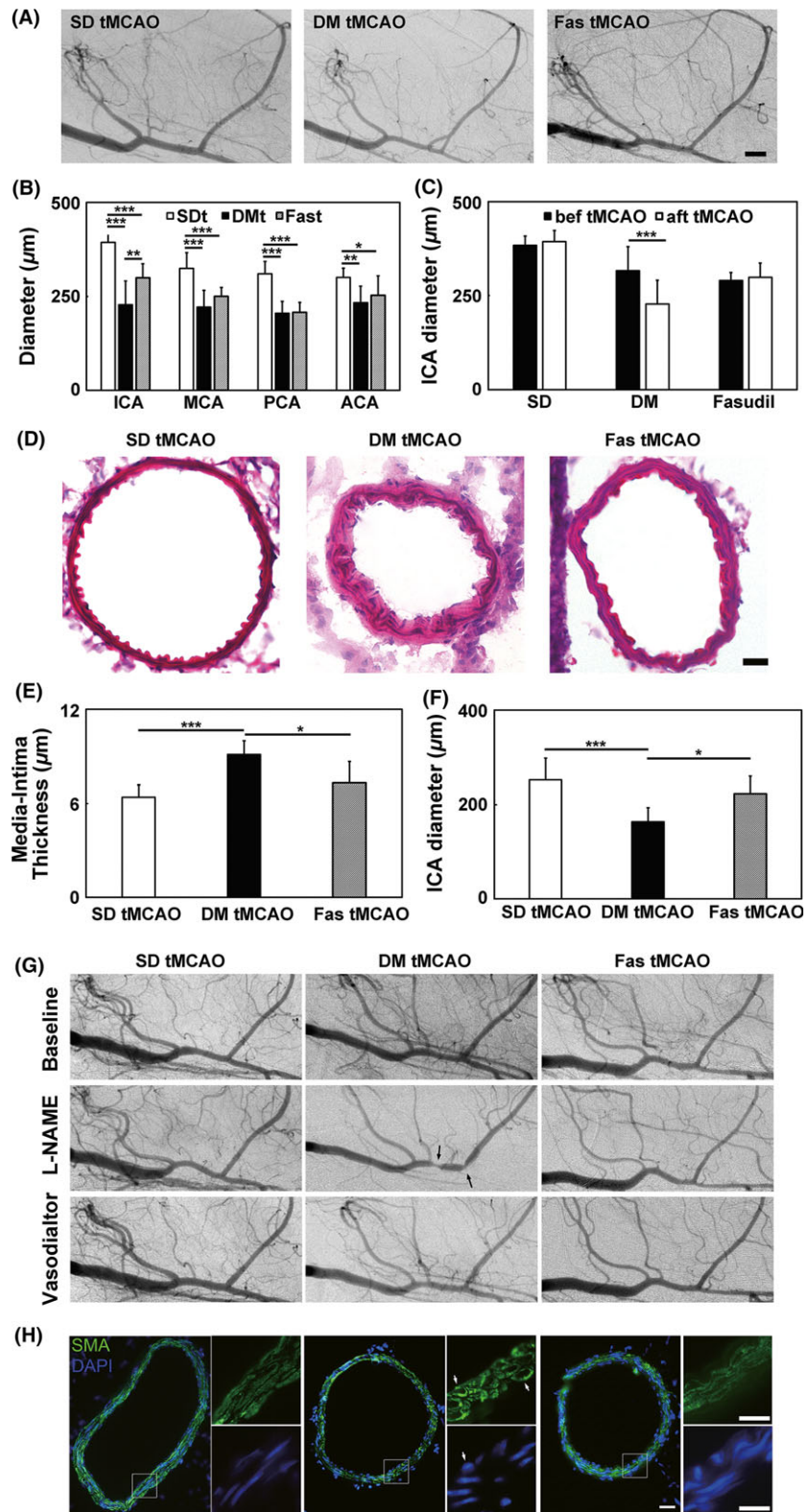
Figure 3 Fasudil treatment partly prevented ischemia-induced arterial constrictions in hyperglycemic rats. (**A**) Synchrotron radiation angiogram (SRA) images of SD, hyperglycemic and fasudil-treated hyperglycemic rats at 1 day after transient middle cerebral artery occlusion (tMCAO). Bar = 1000 μm. (**B**). Bar graph of arterial diameters of ICA, MCA, PCA, and ACA in SD, hyperglycemic and fasudil-treated hyperglycemic rats at 1 day after tMCAO. The three groups were abbreviated as SDt, DMt, and Fast. n = 6–12 per group, values are mean ± SD, *P < 0.05, SDt ACA versus Fast ACA; **P < 0.01, DMt ICA versus Fast ICA; ***P < 0.001, SDt ICA versus DMt ICA, SDt ICA versus Fast ICA, SDt MCA versus DMt MCA, SDt MCA versus Fast MCA, SDt PCA versus DMt PCA, SDt PCA versus Fast PCA. (**C**) Bar graph of arterial diameters of ICA before and after tMCAO. n = 6–12 per group, values are mean ± SD, ***P < 0.001, DM bef tMCAO versus DM aft tMCAO. (**D**) HE staining of ICA. Bar = 10 μm. (**E**) Media–intima thickness of ICA. n = 4–5 per group, values are mean ± SD, *P < 0.05, DM tMCAO versus Fas tMCAO; ***P < 0.001, SD tMCAO versus DM tMCAO. (**F**) Internal diameter of ICA. n = 4–5 per group, values are mean ± SD, *P < 0.05, DM tMCAO versus Fas tMCAO; ***P < 0.001, SD tMCAO versus DM tMCAO. (**G**) SRA images of the SD rats, hyperglycemic and fasudil-treated hyperglycemic rats 1 day after tMCAO at the time before intervention, after L-NAME and vasodilator injection. Black arrow points to focal constrictions. (**H**) SMA immunohistostaining of ICA. White arrow points to the transformed smooth muscle cells. Bar = 20 μm.

only tested vascular constriction and relaxation function, which represent impaired cerebrovascular elasticity in diabetic rats. Similarly, because diabetic endothelial injury was widely studied [5,39], we studied the basal diameter of arteries but not capillaries. Our result is the first to demonstrate that stroke aggravated vascular stenosis through enhancing vascular dysfunction in diabetic
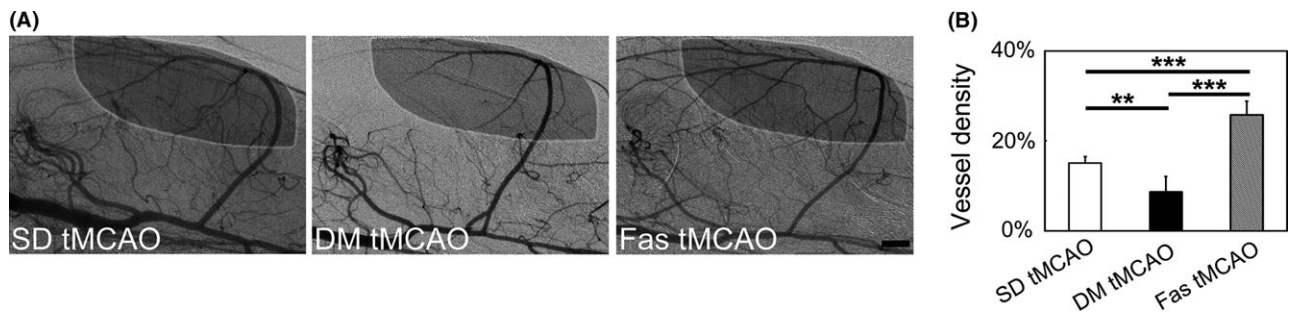
Figure 4 Fasudil treatment ameliorated ischemia-induced arterial constrictions in hyperglycemic rats. (**A**) Representative SRA images indicating vessel density calculation. White circle showed the area for measurement. (**B**) Bar graph of vessel density in cerebral cortex in SD, hyperglycemic and fasudil-treated hyperglycemic rats one day after tMCAO. n = 4–8 per group, values are mean ± SD, **$P < 0.01$, SD tMCAO versus DM tMCAO; ***$P < 0.001$, DM tMCAO versus Fas tMCAO, SD tMCAO versus Fas tMCAO. Bar = 1 mm.

rats and may impair cerebrovascular regulation after stroke, which was supported by decreased cortical vessel perfusion density in living diabetic rats. This might explain why the effects of increased cerebral vessels in diabetic rats were functionally limited and cannot promote cerebral blood flow after stroke [7,31,40]. We did not observe any obvious atherosclerotic changes of cerebral arteries in diabetic rats at 4 weeks after STZ injection. The mean arterial pressure of diabetic rats dropped at 4 weeks after STZ injection and previous study proved that vascular dysfunction could be an important reason [17]. Dynamic vascular dysfunction might be the cause of arterial stenosis of the circus Willis and the decrease of perfusion arterioles in cortex. The decrease of cortical vessel perfusion density was in agreement with previous report of decreased vessel recruitment of coronary arteries in diabetic rats [17]. Other studies have also reported that impaired cerebrovascular regulation is detrimental to the progression of lesion and ensuing hemorrhage and edema [41]. Therefore, the evidence from our study further supported the necessity of improving vascular function in diabetics.

We found that prolonged fasudil treatment before stroke ameliorated vascular dysfunction and greatly improved the prognosis of stroke, indicating that Rho-kinase may be involved in diabetic complications. Previous study has demonstrated that diabetes can enhance RhoA activity in vascular endothelial cells [20,42] and Rho-kinase activity is correlated with diabetic vascular dysfunction [19,22,39]. The activation of Rho/Rho-kinase pathway contributes to endothelial dysfunction through negative regulation of endothelial NOS [43,44], which plays an important role in worsening stroke outcome [13]. ROCK knockout attenuates vascular endothelial dysfunction in diabetic mice [42]. Fasudil treatment protected vascular endothelium and improve hemodynamics in the diabetic retinopathy [20] and hyperlipidemic mice [24]. The results from our investigation are consistent with the results from these studies.

The recent studies of diabetes-induced vascular changes have various limitations. Some investigated the vascular changes *in vitro* to study the mechanisms of diabetic vascular changes [20,45], at the cost of functional changes of cerebral vessels. Others studied the vascular responses of cerebral arterioles in cortex [11,19], while the connections of large vessels and small vessels are unclear. SRA provided the tool for investigating the cerebrovascular changes of the whole brain as well as the dynamic

functional responses of vessels right after ischemic stroke in living animals.

In general, MAP was normal when measuring 8 weeks or 2–3 months after diabetes induction [7,11]. Interestingly, other study also found that MAP decreased 3 weeks after diabetes induction [17]. Autoregulatory alterations in nervous and vascular tone should be the main reason for the change of MAP [46]. We believed that the MAP change may be related to the animal model. Although MAP decreased in the diabetic rats, SBP increased at 4 and 6 weeks, which may be caused by the large artery constriction.

There are several limitations in our study. Firstly, we do not apply permanent MCAO model, which may be considered more translational and informative. Although permanent MCAO is a good model for translational study, transient MCAO, which models ischemia–reperfusion injury in animals, is also important for exploring the role of reperfusion injury on vascular function. Many studies about improving vascular reactivity in diabetic rats to reduce stroke damage were performed on tMCAO. So, we choose tMCAO to model stroke in hyperglycemic rats. Secondly, from clinical reality, glycemic control should be applied to our study. Although tight glycemic control was adopted by clinical practice, many basic researches did not apply it [11,34]. Conventional strategies to control blood glucose level, like insulin and exercise, have been found to contribute to improving vascular function and reducing stroke damage. Therefore, we did not conduct glycemic control. Thirdly, there was no real CBF data. We agree that CBF data could support the results of vascular density. But conventional measurements of CBF like Laser Doppler flowmetry and new techniques such as laser speckle imaging and two photon imaging could only be applied to detect the surface blood flow but not whole MCA territory blood supply in living rats. In contrast, our results reflected the whole brain vascular density, so we did not use these data to support our results. Fourthly, benefit was only seen by prestroke treatment of fasudil, not poststroke. It would be better to compare the effects of fasudil between prestroke and poststroke treatment. Study of the effects of fasudil on acute treatment has been reported previously but the study of its effect on prestroke treatment was unclear. Therefore, we focused on prestroke preventional treatment. Lastly, underlying mechanisms of fasudil beneficial effects were not investigated. Studies demonstrated that fasudil ameliorated diabetes-induced

vascular damages through Rho-kinase inhibition [7,42]. Therefore, further investigation of the pathways involved and mechanism of fasudil function are needed. As Rho-kinase activity is correlated with diabetic vascular dysfunction and ROCK knockout attenuates vascular endothelial dysfunction in diabetic mice [39,42], we postulate that Rho-kinase inhibition contributed to the restoration of vascular function.

Conclusion

Our dynamic angiographic data demonstrated that diabetes could impair the cerebral arterial reactivity. Prolonged fasudil treatment could attenuate arterial dysfunction and improve the

prognosis of ischemic stroke by affecting both the large and small vasculature.

Acknowledgments

Conflict of Interest

The authors declare no conflict of interest.

References

1. Grundy SM, Benjamin IJ, Burke GL, et al. Diabetes and cardiovascular disease: A statement for healthcare professionals from the American Heart Association. *Circulation* 1999;**100**:1134–1146.

2. Alvarez-Sabin J, Molina CA, Montaner J, et al. Effects of admission hyperglycemia on stroke outcome in reperfused tissue plasminogen activator–treated patients. *Stroke* 2003;**34**:1235–1241.

3. Ergul A, Kelly-Cobbs A, Abdalla M, Fagan SC. Cerebrovascular complications of diabetes: Focus on stroke. *Endocr Metab Immune Disord Drug Targets* 2012;**12**:148–158.

4. Yan T, Chopp M, Ning R, Zacharek A, Roberts C, Chen J. Intracranial aneurysm formation in type-one diabetes rats. *PLoS ONE* 2013;**8**:e67949.

5. Cosentino F, Rubattu S, Savoia C, Venturelli V, Pagannonne E, Volpe M. Endothelial dysfunction and stroke. *J Cardiovasc Pharmacol* 2001;**38**(Suppl 2):S75–S78.

6. Li W, Prakash R, Kelly-Cobbs AI, et al. Adaptive cerebral neovascularization in a model of type 2 diabetes: Relevance to focal cerebral ischemia. *Diabetes* 2010;**59**:228–235.

7. Poittevin M, Bonnin P, Pimpie C, et al. Diabetic microangiopathy: Impact of impaired cerebral vasoreactivity and delayed angiogenesis after permanent middle cerebral artery occlusion on stroke damage and cerebral repair in mice. *Diabetes* 2015;**64**:999–1010.

8. Suwaidi JA, Hamasaki S, Higano ST, Nishimura RA, Holmes DR Jr, Lerman A. Long-term follow-up of patients with mild coronary artery disease and endothelial dysfunction. *Circulation* 2000;**101**:948–954.

9. Papaioannou GI, Kasapis C, Seip RL, et al. Value of peripheral vascular endothelial function in the detection of relative myocardial ischemia in asymptomatic type 2 diabetic patients who underwent myocardial perfusion imaging. *J Nucl Cardiol* 2006;**13**:362–368.

10. Nitenberg A, Pham I, Antony I, Valensi P, Attali JR, Chemla D. Cardiovascular outcome of patients with abnormal coronary vasomotion and normal coronary arteriography is worse in type 2 diabetes mellitus than in arterial hypertension: A 10 year follow-up study. *Atherosclerosis* 2005;**183**:113–120.

11. Trauernicht AK, Sun H, Patel KP, Mayhan WG. Enalapril prevents impaired nitric oxide synthase-dependent dilatation of cerebral arterioles in diabetic rats. *Stroke* 2003;**34**:2698–2703.

12. Romero MJ, Platt DH, Tawfik HE, et al. Diabetes-induced coronary vascular dysfunction involves increased arginase activity. *Circ Res* 2008;**102**:95–102.

13. Li Q, Atochin D, Kashiwagi S, et al. Deficient eNOS phosphorylation is a mechanism for diabetic vascular dysfunction contributing to increased stroke size. *Stroke* 2013;**44**:3183–3188.

14. Sachidanandam K, Harris A, Hutchinson J, Ergul A. Microvascular versus macrovascular dysfunction in type 2 diabetes: Differences in contractile responses to endothelin-1. *Exp Biol Med (Maywood)* 2006;**231**:1016–1021.

15. Zhong MF, Shen WL, Wang J, et al. Paradoxical effects of streptozotocin-induced diabetes on endothelial dysfunction in stroke-prone spontaneously hypertensive rats. *J Physiol* 2011;**589**:5153–5165.

16. Yuan F, Lin X, Guan Y, et al. Collateral circulation prevents masticatory muscle impairment in rat middle cerebral artery occlusion model. *J Synchrotron Radiat* 2014;**21**:1314–1318.

17. Jenkins MJ, Edgley AJ, Sonobe T, et al. Dynamic synchrotron imaging of diabetic rat coronary microcirculation in vivo. *Arterioscler Thromb Vasc Biol* 2012;**32**:370–377.

18. Chrissobolis S, Sobey CG. Recent evidence for an involvement of rho-kinase in cerebral vascular disease. *Stroke* 2006;**37**:2174–2180.

19. Didion SP, Lynch CM, Baumbach GL, Faraci FM. Impaired endothelium-dependent responses and enhanced influence of Rho-kinase in cerebral arterioles in type II diabetes. *Stroke* 2005;**36**:342–347.

20. Arita R, Hata Y, Nakao S, et al. Rho kinase inhibition by fasudil ameliorates diabetes-induced microvascular damage. *Diabetes* 2009;**58**:215–226.

21. Srivastava K, Shao B, Bayraktutan U. PKC-beta exacerbates in vitro brain barrier damage in hyperglycemic settings via regulation of RhoA/Rho-kinase/MLC2 pathway. *J Cereb Blood Flow Metab* 2013;**33**:1928–1936.

22. Pearson JT, Jenkins MJ, Edgley AJ, et al. Acute Rho-kinase inhibition improves coronary dysfunction in vivo, in the early diabetic microcirculation. *Cardiovasc Diabetol* 2013;**12**:111.

23. Shin HK, Salomone S, Potts EM, et al. Rho-kinase inhibition acutely augments blood flow in focal cerebral ischemia via endothelial mechanisms. *J Cereb Blood Flow Metab* 2007;**27**:998–1009.

24. Shin HK, Huang PL, Ayata C. Rho-kinase inhibition improves ischemic perfusion deficit in hyperlipidemic mice. *J Cereb Blood Flow Metab* 2014;**34**:284–287.

25. van Nieuw Amerongen GP, Beckers CM, Achekar ID, Zeeman S, Musters RJ, van Hinsbergh VW. Involvement of Rho kinase in endothelial barrier maintenance. *Arterioscler Thromb Vasc Biol* 2007;**27**:2332–2339.

26. Guan SJ, Ma ZH, Wu YL, et al. Long-term administration of fasudil improves cardiomyopathy in streptozotocin-induced diabetic rats. *Food Chem Toxicol* 2012;**50**:1874–1882.

27. Tang Y, Wang J, Lin X, et al. Neural stem cell protects aged rat brain from ischemia-reperfusion injury through neurogenesis and angiogenesis. *J Cereb Blood Flow Metab* 2014;**34**:1138–1147.

28. Lin X, Miao P, Wang J, et al. Surgery-related thrombosis critically affects the brain infarct volume in mice following transient middle cerebral artery occlusion. *PLoS ONE* 2013;**8**:e75561.

29. Cipolla MJ, Porter JM, Osol G. High glucose concentrations dilate cerebral arteries and diminish myogenic tone through an endothelial mechanism. *Stroke* 1997;**28**:405–410; discussion 410–401.

30. Jarajapu YP, Guberski DL, Grant MB, Knot HJ. Myogenic tone and reactivity of cerebral arteries in type II diabetic BBZDR/Wor rat. *Eur J Pharmacol* 2008;**579**:298–307.

31. Kelly-Cobbs AI, Prakash R, Coucha M, et al. Cerebral myogenic reactivity and blood flow in type 2 diabetic rats: Role of peroxynitrite in hypoxia-mediated loss of myogenic tone. *J Pharmacol Exp Ther* 2012;**342**:407–415.

32. Arrick DM, Sharpe GM, Sun H, Mayhan WG. Diabetes-induced cerebrovascular dysfunction: Role of poly(ADP-ribose) polymerase. *Microvasc Res* 2007;**73**:1–6.

33. Arrick DM, Sharpe GM, Sun H, Mayhan WG. nNOS-dependent reactivity of cerebral arterioles in Type 1 diabetes. *Brain Res* 2007;**1184**:365–371.

34. Arrick DM, Sun H, Patel KP, Mayhan WG. Chronic resveratrol treatment restores vascular responsiveness of cerebral arterioles in type 1 diabetic rats. *Am J Physiol Heart Circ Physiol* 2011;**301**:H696–H703.

35. Arrick DM, Sharpe GM, Sun H, Mayhan WG. Losartan improves impaired nitric oxide synthase-dependent dilatation of cerebral arterioles in type 1 diabetic rats. *Brain Res* 2008;**1209**:128–135.

36. Mayhan WG, Arrick DM, Patel KP, Sun H. Exercise training normalizes impaired NOS-dependent responses of cerebral arterioles in type 1 diabetic rats. *Am J Physiol Heart Circ Physiol* 2011;**300**:H1013–H1020.

37. Arrick DM, Sun H, Mayhan WG. Influence of exercise training on ischemic brain injury in type 1 diabetic rats. *J Appl Physiol 1985* 2012;**112**:1121–1127.

38. Arrick DM, Yang S, Li C, Cananzi S, Mayhan WG. Vigorous exercise training improves reactivity of cerebral arterioles and reduces brain injury following transient focal ischemia. *Microcirculation* 2014;**21**:516–523.

39. Sena CM, Pereira AM, Seica R. Endothelial dysfunction – a major mediator of diabetic vascular disease. *Biochim Biophys Acta* 2013;**1832**:2216–2231.

40. Ye X, Chopp M, Cui X, et al. Niaspan enhances vascular remodeling after stroke in type 1 diabetic rats. *Exp Neurol* 2011;**232**:299–308.

41. Dohmen C, Bosche B, Graf R, et al. Identification and clinical impact of impaired cerebrovascular autoregulation in patients with malignant middle cerebral artery infarction. *Stroke* 2007;**38**:56–61.

42. Yao L, Chandra S, Toque HA, et al. Prevention of diabetes-induced arginase activation and vascular dysfunction by Rho kinase (ROCK) knockout. *Cardiovasc Res* 2013;**97**:509–519.

43. Budzyn K, Marley PD, Sobey CG. Targeting Rho and Rho-kinase in the treatment of cardiovascular disease. *Trends Pharmacol Sci* 2006;**27**:97–104.

44. Shiga N, Hirano K, Hirano M, Nishimura J, Nawata H, Kanaide H. Long-term inhibition of RhoA attenuates vascular contractility by enhancing endothelial NO production in an intact rabbit mesenteric artery. *Circ Res* 2005;**96**:1014–1021.

45. Mishiro K, Imai T, Sugitani S, et al. Diabetes mellitus aggravates hemorrhagic transformation after ischemic stroke via mitochondrial defects leading to endothelial apoptosis. *PLoS ONE* 2014;**9**:e103818.

46. Westerhof N, Boer C, Lamberts RR, Sipkema P. Cross-talk between cardiac muscle and coronary vasculature. *Physiol Rev* 2006;**86**:1263–1308.